

Calculation of the volume pinning force in MgB₂ superconductors

M. Eisterer*

Atomic Institute of the Austrian Universities, Vienna University of Technology, 1020 Vienna, Austria

(Received 8 February 2008; revised manuscript received 3 April 2008; published 28 April 2008)

The field dependence of the volume pinning force in anisotropic polycrystalline superconductors is calculated for various well established pinning models. The anisotropy substantially changes the field dependence of the volume pinning force and shifts its maximum to significantly lower reduced fields. A scaling procedure that allows the identification of the dominant pinning mechanism from the peak position is proposed.

DOI: 10.1103/PhysRevB.77.144524

PACS number(s): 74.70.Ad, 74.25.Qt, 74.81.Bd, 74.25.Sv

I. INTRODUCTION

The intrinsic anisotropy of the magnetic properties of magnesium diboride¹⁻⁵ leads to a peculiar current transport in polycrystalline materials.⁶ The supercurrents never flow homogeneously since the differently oriented grains attain different properties when a magnetic field is applied. This field induced inhomogeneity is unique to MgB₂ conductors so far since conventional superconductors are (nearly) isotropic and high temperature superconductors have to be textured in order to avoid the weak link problem of high angle grain boundaries.⁷

Clean grain boundaries do not limit the current flow in magnesium diboride⁸⁻¹⁰ but act as efficient pinning centers¹¹⁻¹⁶ and enable high currents in untextured polycrystalline filaments of wires or tapes. Nevertheless, secondary phases often cover the surface of the grains,¹⁷⁻¹⁹ partly block the current flow, and reduce the effective area over which the supercurrents flow.²⁰ This problem is amplified by voids or secondary phases and enhances current percolation, which is a natural consequence of the magnetic anisotropy.²¹

The peculiar current transport in MgB₂ significantly alters the field dependence of the critical current density^{6,21} and, consequently, of the volume pinning force density, $\mathbf{J} \times \mathbf{B}$. The latter was recently used to derive information on the pinning mechanism^{11,22} in the same way as in isotropic or textured superconductors. If a single pinning mechanism prevails in these materials, the field dependence of the volume pinning force density F_p can often be described by simple power laws, $F_p \propto b^m(1-b)^n$, where b denotes the reduced field, $b=B/B_{\text{irr}}$, and B_{irr} is the field where the critical currents and the volume pinning force become zero. The exponents m and n are characteristic for the dominant pinning mechanism.²³ For instance, m is predicted to be 1/2 for grain boundary pinning or 1 for normal conducting point pinning centers, with $n=2$ in both cases. A single pinning mechanism can be easily identified by comparing the volume force density with various predictions. This simple procedure is not applicable to untextured, anisotropic materials, such as wires or tapes of MgB₂. In this paper, it will be shown that the peak in the field dependence of the volume pinning force is significantly shifted to lower reduced fields by the anisotropy. A scaling procedure that relates the peak position to the underlying pinning mechanism will be presented.

II. MATHEMATICAL MODEL

The critical current densities were calculated by numerical evaluation of⁶

$$J_c = \int_0^{J_{\text{max}}} \left(\frac{p(J) - p_c}{1 - p_c} \right)^{1.79} dJ. \quad (1)$$

$p(J)$ denotes the fraction of grains with critical current densities above J . J_{max} is given by the condition $p(J_{\text{max}}) = p_c$. The percolation threshold p_c is defined as the minimum fraction of a superconducting material for a continuous superconducting current path. Randomly oriented grains [$p(\alpha > \theta) = \cos(\theta)$,²⁴ with α and θ being the angles with respect to the crystallographic c axis] were assumed for the calculation of $p(J)$. The field dependence of the critical currents is given by the actual pinning model,

$$J_c(B) \propto B^{m-1} \left(1 - \frac{B}{B_{\text{norm}}} \right)^n \quad (2)$$

for $B < B_{\text{norm}}$ and $J_c = 0$ for $B > B_{\text{norm}}$. The critical current anisotropy was modeled by the scaling approach proposed by Blatter *et al.*,²⁵ i.e., B was multiplied by $\sqrt{\cos^2 \theta + \gamma^{-2} \sin^2 \theta}$, where γ denotes the anisotropy of the upper critical field, B_{c2}^{ab}/B_{c2}^c , and θ is the angle between the applied magnetic field and the crystallographic c axis. The field B_{norm} then refers to the irreversibility field for $H \parallel c$, B_{irr}^c . [B_{norm} is used to distinguish this *intrinsic* irreversibility field from the macroscopic irreversibility field B_{irr} , cf. Eq. (3)]. The scaling approach implicitly assumes that the angular dependence of the magnetic properties follows the prediction of the anisotropic Ginzburg–Landau theory,²⁶ which was found to be a good approximation for MgB₂ at intermediate and high magnetic fields.^{1,3,27,28} The two band nature of superconductivity in MgB₂ leads to deviations only at low fields, where both bands significantly contribute to the superfluid density.^{4,21,29-34} However, the contribution of the π band to the critical currents should also be small at low fields³⁵ because of the small condensation energy $E_{c,\pi}$.³³ It was demonstrated that the one band assumption successfully describes the critical currents at all fields.⁶ Furthermore, the critical current density was multiplied by B to obtain F_p ; thus, any influence of the π band at small fields is further suppressed.

The field B_{irr}^c [B_{norm} in Eq. (2)] is *a priori* unknown in polycrystalline samples and rather difficult to determine. It is $B_{\text{irr}}^{ab}/\gamma$ (anisotropic scaling) that was chosen freely since all fields were normalized by the macroscopic irreversibility field,²⁴

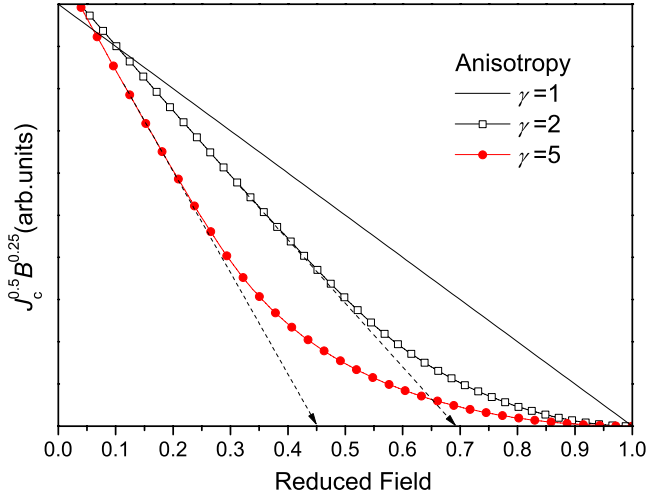


FIG. 1. (Color online) Theoretical Kramer plot of three polycrystalline superconductors with different anisotropies. The percolation threshold p_c was fixed to 0.25.

$$B_{\text{irr}} = \frac{B_{\text{irr}}^{ab}}{\sqrt{(\gamma^2 - 1)p_c^2 + 1}}. \quad (3)$$

Above B_{irr} , a continuous macroscopic supercurrent path does not exist any longer, although a significant fraction of the grains remain superconducting with $J_c > 0$ up to B_{irr}^{ab} , which is always larger than B_{irr} .

Equation (3) was originally derived with the simplification $B_{\text{irr}}^{ab} = B_{c2}^{ab}$, but it can be extended to the general case by simply replacing B_{c2}^{ab} with B_{irr}^{ab} . It should be noted that the scaling laws for the volume pinning force were also derived under the assumption $B_{\text{irr}} = B_{c2}$.²³ It is not obvious that they remain unchanged if B_{irr} is much below B_{c2} . However, the (intrinsic) irreversibility field is always close to the upper critical field in MgB_2 (Refs. 14 and 36–38) and in the conventional superconductors.

Finally, the volume pinning force density was normalized to its maximum.

III. RESULTS AND DISCUSSION

A. Kramer plot

The anisotropy not only changes the field dependence of the critical currents and of the volume pinning force but also the Kramer plot (i.e., $J_c^{1/2} B^{1/4}$ vs B), as demonstrated in Fig. 1. Grain boundary pinning [$F_p \propto b^{1/2}(1-b)^2$] was assumed, resulting in a linear behavior in the isotropic case (line graph in Fig. 1), which can be used to reliably determine B_{irr} . This was also tried for MgB_2 ,^{11,22} although the linear behavior is restricted to fields well below B_{irr} and linear extrapolation of this low field region leads to a significant underestimation of B_{irr} (arrows in Fig. 1). Since the currents become very small at high fields and very slowly approach zero, the Kramer plot is not suitable for determining B_{irr} in polycrystalline MgB_2 . The original benefit of the Kramer representation, namely, a well defined (linear) high field behavior, completely disappears in polycrystalline MgB_2 .

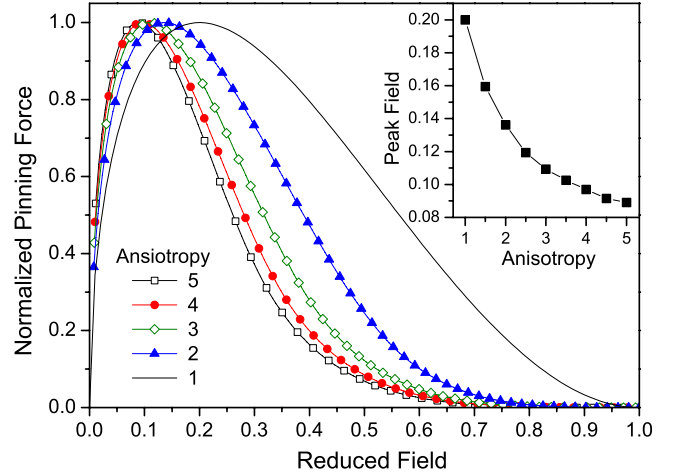


FIG. 2. (Color online) Influence of the anisotropy on the volume pinning force for grain boundary pinning and $p_c = 0.25$. Inset: Position of the maximum as a function of anisotropy.

B. Volume pinning force

The position of the maximum of the volume pinning force depends not only on the pinning model but also on the anisotropy γ and on the percolation threshold p_c . We start by considering grain boundary pinning since this mechanism is dominant in many samples.^{11,12,15,16,39} The influence of the anisotropy on the volume pinning force is demonstrated in Fig. 2 for $p_c = 0.25$. The peak continuously shifts to lower (reduced) fields with increasing anisotropy. The anisotropy of MgB_2 strongly depends on the purity of the material⁴⁰ and can change between about 6 in the clean limit and 1 in the dirty limit.²¹ However, it is expected to be between 4 and 5 in most samples, corresponding to a transition temperature T_c of about 33–38 K.²¹ The peak position only slightly changes in this region from $b = 0.097$ to 0.089.

In the isotropic case, the peak position can be easily calculated from the power law $b^m(1-b)^n$, which has its maximum at $m/(m+n)$. A value of 0.2 is obtained for grain boundary pinning ($m = 1/2$ and $n = 2$).²³ Thus, the peak field in most MgB_2 samples is reduced by a factor of more than 2.

The volume pinning force becomes very small at reduced fields above about 0.7 (but remains finite up to $b = 1$, which is hardly visible in Fig. 2) if the anisotropy is above 2. Only highly percolative currents exist at high fields and the irreversibility field is very hard to determine from such plots. Nevertheless, B_{irr} is crucial for the normalization of the magnetic field and, consequently, for the reduced peak field.

The changes in F_p due to changes in the percolation threshold are comparatively small (Fig. 3) since p_c is expected to vary only between 0.2 and 0.3 in three-dimensional systems.^{6,41} The percolation threshold mainly depends on the number of connections between the grains; thus, clean dense samples have a comparatively small p_c and porous or dirty samples with a large amount of secondary phases have a larger p_c .^{21,42}

The peak field only changes from 0.09 for $p_c = 0.2$ to 0.103 for $p_c = 0.3$ in the case of a typical anisotropy of 4 (inset in Fig. 3). It might be surprising at first that a smaller percolation threshold shifts the peak to lower reduced fields,

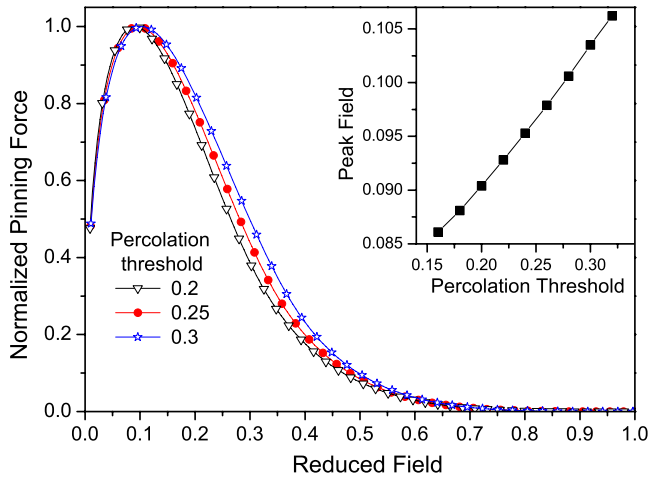


FIG. 3. (Color online) Change in the volume pinning force with the percolation threshold for $\gamma=4$.

but this is just a consequence of the increase in the irreversibility field. In fact, the absolute value of the peak field increases as p_c decreases (for fixed B_{irr}^{ab}), but this is overcompensated by the enhancement in B_{irr} [cf. Eq. (3)].

Another important pinning mechanism in MgB_2 is pinning by small (pointlike) normal conducting inclusions³⁹ ($m=1$ and $n=2$).²³ The corresponding peak field is $1/3$ in the isotropic case, which is larger than that for grain boundary pinning ($1/5$). The latter remains true for anisotropic superconductors (solid symbols in Fig. 4). Similar to grain boundary pinning, the peak field is reduced by a factor of more than 2 ($b_{\text{peak}}=0.158$) for $\gamma=4$ and $p_c=0.25$ (typical values for MgB_2). The differences in the peak position of the different pinning mechanisms can be used, in principle, in determining the dominant pinning mechanism. Unfortunately, γ and p_c have to be known, at least approximately, for this purpose. In order to avoid this problem, a modified scaling procedure is proposed in Sec. III C.

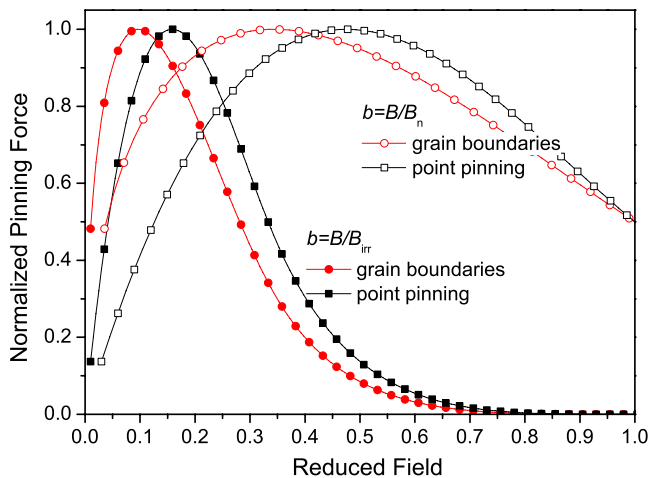


FIG. 4. (Color online) Comparison of the field dependence of the volume pinning force resulting from grain boundary pinning (circles) and from point pinning (squares). The solid and open symbols refer to normalization of B by B_{irr} and by B_n (see text), respectively.

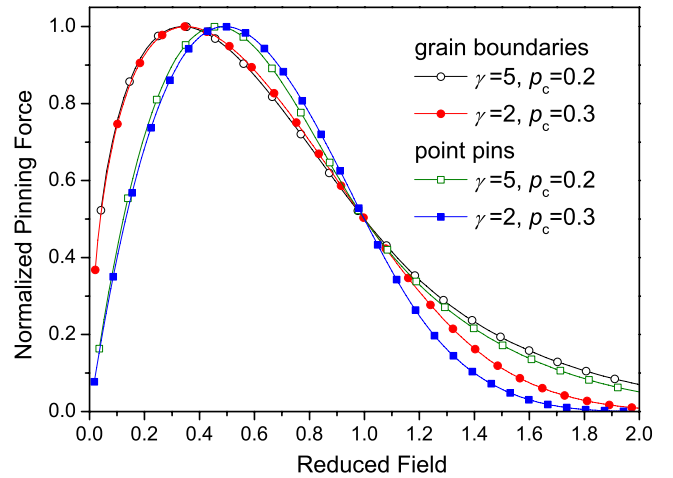


FIG. 5. (Color online) Demonstration of the modified scaling procedure. The influence of γ and p_c is strongly reduced for $B/B_n < 1$.

C. Modified scaling procedure

Figure 5 presents the volume pinning force as a function of $b_n=B/B_n$. B_n is defined as the field wherein F_p drops to 50% of its maximum at fields above the peak field. Two extreme cases are assumed, which are a very clean ($\gamma=5$, $p_c=0.2$, open symbols) and a very dirty ($\gamma=2$, $p_c=0.3$, solid symbols) material. The curves representing grain boundary pinning (circles) nearly collapse below $b_n=1$ and significant differences exist only at higher fields. The position of the peak field only shifts by about 3% from 0.341 for the clean to 0.352 for the dirty material. This difference is smaller than the usual deviations from the predicted behavior in textured MgB_2 superconductors (films),^{14,43,44} which should be identical to that of isotropic superconductors ($B/B_{\text{irr}}=0.2$ for grain boundary pinning).

The difference in the peak position increases to nearly 6% for point pinning and the peak shifts from 0.465 (clean material) to 0.491 (dirty material). However, the assumed values for γ and p_c are limiting cases and the anisotropy and p_c should not vary too significantly in most MgB_2 samples ($\gamma=2$ corresponds to materials with $T_c \approx 20$ K).²¹ It is still easily possible to distinguish between grain boundary pinning and point pinning from just the position of the maximum pinning force (Figs. 4 and 5), which differ by nearly 40%.

The normalization field B_n can be determined much better than B_{irr} since the slope of the volume pinning force is large in this region in contrast to the flat behavior of the volume pinning force or that of the Kramer plot (see Sec. III A) near the field wherein the critical currents finally vanish (within accuracy of the experiment).

The peak position was calculated for other pinning mechanisms (different m and n),²³ assuming $\gamma=4$ and $p_c=0.25$, which are typical for MgB_2 . The results are presented in Table I. The exponent $n=2$ generally refers to normal conducting pins and $n=1$ refers to superconducting pins with properties differing from those of the matrix (Δl or $\Delta \kappa$ pinning). The peak positions refer to B/B_{irr} (third and fourth columns) and to B/B_n (fifth column). The values for isotropic materials are given in the third column for the sake of

TABLE I. Normalized field of the maximum of the volume pinning force for various scaling laws, $F_p \propto b^m(1-b)^n$. The values in columns 3 and 4 refer to normalization by B_{irr} . The values in column 5 were normalized by B_n . $\gamma=4$ and $p_c=0.25$ were assumed in columns 4 and 5.

m	n	Isotropic	Anisotropic	Rescaled
1/2	2	0.2	0.1	0.34
1	2	0.33	0.16	0.47
1/2	1	0.33	0.16	0.42
1	1	0.5	0.23	0.56
3/2	1	0.6	0.28	0.62
2	1	0.67	0.31	0.65

completeness, but they are also an indication of the accuracy of the new scaling procedure. The higher the field wherein the peak occurs in isotropic materials, the larger the influence of γ and p_c is on the peak field, B_{peak}/B_n , and the poorer the scaling behavior is below $b_n < 1$. This was already indicated

by the larger deviations for point pinning than those for grain boundary pinning (Fig. 4).

IV. SUMMARY AND CONCLUSION

It was demonstrated that the field dependence of the volume pinning force is significantly influenced by the intrinsic anisotropy γ in untextured polycrystalline MgB_2 specimens. This complicates the identification of the underlying pinning mechanism. The (normalized) field, wherein the maximum of the volume force occurs in typical MgB_2 samples, decreases by a factor of around 2 compared to that of isotropic or textured samples. The morphology of the material (percolation threshold p_c) was found to only slightly change the volume pinning force. The influence of the *a priori* unknown parameters γ and p_c can be strongly reduced by a modified scaling procedure, thus allowing us to identify the dominant pinning mechanism from the peak position.

ACKNOWLEDGMENT

I wish to thank Harald W. Weber for useful discussions and for critically reading this paper.

*eisterer@ati.ac.at

- ¹M. Angst, R. Puzniak, A. Wisniewski, J. Jun, S. M. Kazakov, J. Karpinski, J. Roos, and H. Keller, Phys. Rev. Lett. **88**, 167004 (2002).
- ²S. L. Bud'ko and P. C. Canfield, Phys. Rev. B **65**, 212501 (2002).
- ³A. Rydh, U. Welp, A. E. Koshelev, W. K. Kwok, G. W. Crabtree, R. Brusetti, L. Lyard, T. Klein, C. Marcenat, B. Kang, K. H. Kim, K. H. P. Kim, H.-S. Lee, and S.-I. Lee, Phys. Rev. B **70**, 132503 (2004).
- ⁴M. Zehetmayer, M. Eisterer, J. Jun, S. M. Kazakov, J. Karpinski, and H. W. Weber, Phys. Rev. B **70**, 214516 (2004).
- ⁵L. Lyard, P. Szabo, T. Klein, J. Marcus, C. Marcenat, K. H. Kim, B. W. Kang, H. S. Lee, and S. I. Lee, Phys. Rev. Lett. **92**, 057001 (2004).
- ⁶M. Eisterer, M. Zehetmayer, and H. W. Weber, Phys. Rev. Lett. **90**, 247002 (2003).
- ⁷H. Hilgenkamp and J. Mannhart, Rev. Mod. Phys. **74**, 485 (2002).
- ⁸D. K. Finnemore, J. E. Ostenson, S. L. Bud'ko, G. Lapertot, and P. C. Canfield, Phys. Rev. Lett. **86**, 2420 (2001).
- ⁹M. Kambara, N. Hari Babu, E. S. Sadki, J. R. Cooper, H. Minami, D. A. Cardwell, A. M. Campbell, and I. H. Inoue, Supercond. Sci. Technol. **14**, L5 (2001).
- ¹⁰D. C. Larbalestier, L. D. Cooley, M. O. Rikel, A. A. Polyanskii, J. Jiang, S. Patnaik, X. Y. Cai, D. M. Feldmann, A. Gurevich, A. A. Squitieri, M. T. Naus, C. B. Eom, E. E. Hellstrom, R. J. Cava, K. A. Regan, N. Rogado, M. A. Hayward, T. He, J. S. Slusky, P. Khalifah, K. Inumaru, and M. Haas, Nature (London) **410**, 186 (2001).
- ¹¹E. Martínez, P. Mikheenko, M. Martínez-López, A. Millán, A. Bevan, and J. S. Abell, Phys. Rev. B **75**, 134515 (2007).
- ¹²X. Song, S. E. Babcock, C. B. Eom, D. C. Larbalestier, K. A.

- Regan, R. J. Cava, S. L. Budko, P. Canfield, and D. K. Finnemore, Supercond. Sci. Technol. **15**, 511 (2002).
- ¹³H. Kitaguchi and T. Doi, Supercond. Sci. Technol. **18**, 489 (2005).
- ¹⁴J. Chen, V. Ferrando, P. Orgiani, A. V. Pogrebnaykov, R. H. T. Wilke, J. B. Betts, C. H. Mielke, J. M. Redwing, X. X. Xi, and Q. Li, Phys. Rev. B **74**, 174511 (2006).
- ¹⁵P. Mikheenko, E. Martínez, A. Bevan, J. S. Abell, and J. L. MacManus-Driscoll, Supercond. Sci. Technol. **20**, S264 (2007).
- ¹⁶H. Sosiati, S. Hata, N. Kuwano, Y. Tomokiyo, H. Kitaguchi, T. Doi, H. Yamamoto, A. Matsumoto, K. Saitoh, and H. Kumakura, Supercond. Sci. Technol. **18**, 1275 (2005).
- ¹⁷R. F. Klie, J. C. Idrobo, N. D. Browning, K. A. Regan, N. S. Rogado, and R. J. Cava, Appl. Phys. Lett. **79**, 1837 (2001).
- ¹⁸D. Eyidi, O. Eibl, T. Wenzel, K. G. Nickel, M. Giovannini, and A. Saccone, Micron **34**, 85 (2003).
- ¹⁹J. Jiang, B. J. Senkowicz, D. C. Larbalestier, and E. E. Hellstrom, Supercond. Sci. Technol. **19**, L33 (2006).
- ²⁰J. M. Rowell, Supercond. Sci. Technol. **16**, R17 (2003).
- ²¹M. Eisterer, Supercond. Sci. Technol. **20**, R47 (2007).
- ²²C. Tarantini, H. U. Aebbersold, C. Bernini, V. Braccini, C. Ferdeghini, U. Gambardella, E. Lehmann, P. Manfrinetti, A. Palenzona, I. Pallecchi, M. Vignolo, and M. Putti, Physica B **463-465**, 211 (2007).
- ²³D. Dew-Hughes, Philos. Mag. **30**, 293 (1974).
- ²⁴M. Eisterer, C. Krutzler, and H. W. Weber, J. Appl. Phys. **98**, 033906 (2005).
- ²⁵G. Blatter, V. B. Geshkenbein, and A. I. Larkin, Phys. Rev. Lett. **68**, 875 (1992).
- ²⁶D. R. Tilley, Proc. Phys. Soc. London **86**, 289 (1965).
- ²⁷L. Lyard, P. Samuely, P. Szabo, T. Klein, C. Marcenat, L. Paulius, K. H. P. Kim, C. U. Jung, H.-S. Lee, B. Kang, S. Choi, S.-I. Lee, J. Marcus, S. Blanchard, A. G. M. Jansen, U. Welp, G.

- Karapetrov, and W. K. Kwok, *Phys. Rev. B* **66**, 180502(R) (2002).
- ²⁸S. L. Prischepa, M. L. Della Rocca, L. Maritato, M. Salvato, R. Di Capua, M. G. Maglione, and R. Vaglio, *Phys. Rev. B* **67**, 024512 (2003).
- ²⁹F. Bouquet, Y. Wang, I. Sheikin, T. Plackowski, A. Junod, S. Lee, and S. Tajima, *Phys. Rev. Lett.* **89**, 257001 (2002).
- ³⁰M. R. Eskildsen, M. Kugler, S. Tanaka, J. Jun, S. M. Kazakov, J. Karpinski, and O. Fischer, *Phys. Rev. Lett.* **89**, 187003 (2002).
- ³¹A. E. Koshelev and A. A. Golubov, *Phys. Rev. Lett.* **90**, 177002 (2003).
- ³²R. Cubitt, M. R. Eskildsen, C. D. Dewhurst, J. Jun, S. M. Kazakov, and J. Karpinski, *Phys. Rev. Lett.* **91**, 047002 (2003).
- ³³M. Eisterer, M. Zehetmayer, H. W. Weber, and J. Karpinski, *Phys. Rev. B* **72**, 134525 (2005).
- ³⁴T. Klein, L. Lyard, J. Marcus, Z. Holanava, and C. Marcenat, *Phys. Rev. B* **73**, 184513 (2006).
- ³⁵E. J. Nicol and J. P. Carbotte, *Phys. Rev. B* **72**, 014520 (2005).
- ³⁶C. Ferdeghini, V. Ferrando, G. Grassano, W. Ramadan, E. Bellingeri, V. Braccini, D. Marré, P. Manfrinetti, A. Palenzona, F. Borgatti, R. Felici, and T.-L. Lee, *Supercond. Sci. Technol.* **14**, 952 (2001).
- ³⁷S. Patnaik, L. D. Cooley, A. Gurevich, A. A. Polyanskii, J. Jiang, X. Y. Cai, A. A. Squitieri, M. T. Naus, M. K. Lee, J. H. Choi, L. Belenky, S. D. Bu, J. Letteri, X. Song, D. G. Schlom, S. E. Babcock, C. B. Eom, E. E. Hellstrom, and D. C. Larbalestier, *Supercond. Sci. Technol.* **14**, 315 (2001).
- ³⁸Z. X. Shi, A. K. Pradhan, M. Tokunaga, K. Yamazaki, T. Tamegai, Y. Takano, K. Togano, H. Kito, and H. Ihara, *Phys. Rev. B* **68**, 104514 (2003).
- ³⁹I. Pallecchi, C. Tarantini, H. U. Aebbersold, V. Braccini, C. Fanciulli, C. Ferdeghini, F. Gatti, E. Lehmann, P. Manfrinetti, D. Marré, A. Palenzona, A. S. Siri, M. Vignolo, and M. Putti, *Phys. Rev. B* **71**, 212507 (2005).
- ⁴⁰C. Krutzler, M. Zehetmayer, M. Eisterer, H. W. Weber, N. D. Zhigadlo, and J. Karpinski, *Phys. Rev. B* **75**, 224510 (2007).
- ⁴¹S. C. van der Marck, *Phys. Rev. E* **55**, 1514 (1997).
- ⁴²M. Eisterer, K. R. Schöpl, H. W. Weber, M. D. Sumption, and M. Bhatia, *IEEE Trans. Appl. Supercond.* **17**, 2814 (2007).
- ⁴³M. Haruta, T. Fujiyoshi, T. Sueyoshi, K. Miyahara, T. Doi, H. Kitaguchi, S. Awaji, and K. Watanabe, *Supercond. Sci. Technol.* **18**, 1460 (2005).
- ⁴⁴A. Gupta, H. Narayan, D. Astill, D. Kanjilal, C. Ferdeghini, M. Paranthaman, and A. V. Narlikar, *Supercond. Sci. Technol.* **16**, 951 (2003).